

## Magnetic-Compton-scattering study of spin moments in $\text{UFe}_2$

P. K. Lawson, M. J. Cooper, and M. A. G. Dixon

*Department of Physics, University of Warwick, Coventry CV4 7AL, United Kingdom*

D. N. Timms

*Division of Physics, University of Portsmouth, Portsmouth PO1 2DZ, United Kingdom*

E. Zukowski

*Institute of Physics, University of Warsaw Branch in Bialystok, 15-424 Bialystok, Poland*

F. Itoh and H. Sakurai

*Department of Electrical and Electronic Engineering, Gunma University, Kiryu 376, Japan*

(Received 10 March 1997)

Spin moments were derived from the magnetic-Compton profile of  $\text{UFe}_2$ , which was measured using 59.38-keV circularly polarized synchrotron radiation from the Accumulation Ring Source at KEK, Japan. Although the net moment on the uranium site is no more than a tenth of a Bohr magneton, the individual spin and orbital moments, which are coupled antiparallel, are much larger and it is the spin moment that can be determined in magnetic-Compton scattering. The data have been analyzed in terms of the U  $5f$ , Fe  $3d$  and delocalized spin moments. The observed uranium- $5f$  spin moment is less than half (i.e.,  $<0.25\mu_B$ ) and the diffuse spin moment more than double (i.e.,  $>0.20\mu_B$ ) those predicted from theory. These values compare favorably with those deduced from neutron measurements of the total magnetization. [S0163-1829(97)01630-5]

### I. INTRODUCTION

Below 160 K  $\text{UFe}_2$  is a soft ferromagnet, which crystallizes in the cubic fcc Laves phase and has low magnetic anisotropy similar to that of pure iron.<sup>1</sup> Interest in it arises from the fact that the total moment on the uranium site is very small ( $\ll 0.1\mu_B$ ) as was first deduced from neutron-diffraction experiments two to three decades ago.<sup>2,3</sup> The origin of this anomalously small moment lies in the near-perfect cancellation of the spin and orbital moments which are predicted to be substantial ( $\sim 0.5\mu_B$ ). This leads, in turn, to an unusual magnetic form factor which does not peak at zero-momentum transfer,<sup>4</sup> a fact that was not appreciated in the earliest investigations. *Ab initio* spin-polarized band calculations were made by Brooks *et al.* in 1988;<sup>5</sup> these confirmed the itinerant nature of the U  $5f$  electrons. The inclusion of spin-orbit coupling led to a reduced orbital moment and a better description of the pressure dependence of the moment. They predicted the  $5f$  moments in  $\text{UFe}_2$  to have a ratio,  $-\mu_L/\mu_S$ , of approximately unity in contrast to the value of approximately 2.3 calculated for the  $5f$  electrons in an isolated ion, as determined from spin-orbit coupling. This difference arises from a reduced orbital moment which suggests that the  $5f$  electrons are itinerant and that there is hybridization of  $5f$  and  $3d$  electrons. The proximity of the  $5f$  bands to the Fermi energy also suggests hybridization between the  $5f$  and conduction electron states. The reduction of the orbital moment on an actinide atom is accompanied by a reduction of the spin moment on the transition-metal site to as little as one-third of its value in the pure metal. The moments calculated by Brooks *et al.*<sup>5</sup> are depicted in Fig. 1 and listed in Table I.

A polarized neutron study<sup>4,6</sup> confirmed the near zero mo-

ment on the uranium site, ascribed this to the antiparallel coupling of spin and orbital moments, and showed that this was responsible for the anomalous form factor drop off at low-momentum transfer. They also pointed out that the non-stoichiometric samples used in the early studies<sup>2,3</sup> would have possessed smaller moments. However, the magnitude of the uranium spin and orbital moments that they deduced are approximately half those predicted as can be seen in the table; there is also a significant disagreement between experiment and theory over the size of the Fe  $3d$  and the itinerant

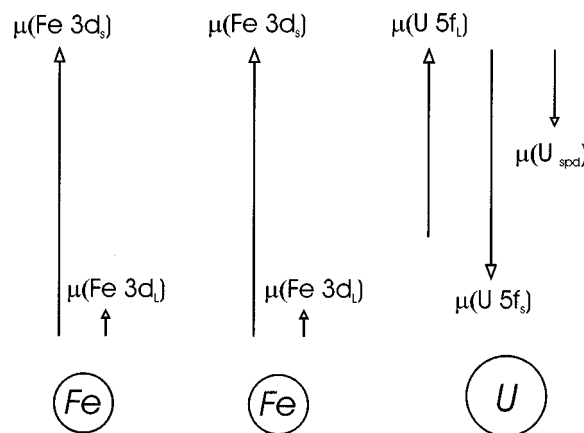


FIG. 1. A diagrammatic representation of the partial magnetic moments in  $\text{UFe}_2$  calculated by self-consistent spin-polarized band theory (Ref. 5): the arrows are to scale approximately (numerical values for the spin moments are listed in the table). For the sake of clarity the calculated  $4sp$  moment on Fe of  $0.02\mu_B$  has not been represented and the  $sp$  and  $d$  spin moments on the uranium site have been added together (they have a combined value of  $-0.13\mu_B$ ).

TABLE I. Magnetic moments in UFe<sub>2</sub>. All values are in Bohr magnetons; orbital moments are not measured in the Compton study, and the Fe3*d* moment plus the diffuse (*spd*) moment are not measured by circular dichroism.

| Magnetic moments $\mu_B$     | Compton free fit results | Compton 2–10 a.u. results | MXCD <sup>10</sup> results | Neutron data <sup>6</sup> | Theoretical prediction <sup>5</sup> |
|------------------------------|--------------------------|---------------------------|----------------------------|---------------------------|-------------------------------------|
| Spin U5 <i>f</i>             | −0.20(9)                 | −0.06(8)                  | −0.20(2)                   | −0.22(2)                  | −0.58                               |
| Spin Fe3 <i>d</i> (per atom) | 0.52(5)                  | 0.46(5)                   | ---                        | 0.59(3)                   | 0.73                                |
| <i>spd</i> itinerant         | −0.22(1)                 | −0.23(1)                  | ---                        | −0.25(2)                  | −0.09                               |
| Orbital U5 <i>f</i>          | ---                      | ---                       | 0.21(2)                    | 0.23(2)                   | 0.47                                |

moment, the former being three-quarters of the calculated value while the latter is almost three times larger. Magnetic moments in the actinides were reviewed from experimental<sup>7,8</sup> and theoretical<sup>9</sup> viewpoints in articles which appeared in 1991.

Very recently<sup>10</sup> the spin and orbital moments on the uranium site in UFe<sub>2</sub> have been deduced from circular dichroism data by using sum rules.<sup>11,12</sup> Those data are also included in the table and will be discussed later. Dichroism studies are, by their nature, element specific; therefore, no information is forthcoming from Ref. 10 on the Fe or itinerant moments.

Neutrons probe the total site magnetization, which in the case of uranium in UFe<sub>2</sub> is extremely small. On the other hand, it has been shown that spin magnetization alone is measured in magnetic-Compton-scattering experiments,<sup>13</sup> a result that has recently been supported theoretically.<sup>14,15</sup> Thus the relatively large spin moments can be studied.

Magnetic Compton scattering with circularly polarized sources was first demonstrated in 1976,<sup>16</sup> and developed with synchrotron radiation from 1986 onwards.<sup>17</sup> A review of the topic has recently appeared.<sup>18</sup> The Compton technique is an incoherent scattering process, therefore the term linear in electron spin which gives rise to the signal measured in these studies is only nonzero for ferro- and ferrimagnets. During the course of a series of experiments on the rare-earth ferrimagnet HoFe<sub>2</sub>,<sup>19,20</sup> it became clear that site-specific information about spin moments can be extracted from magnetic Compton data by utilizing the characteristically different electron momentum distributions on the rare-earth and transition-metal atomic sites. The temperature variation of the moments can also be followed.<sup>21,22</sup> Since the spin-dependent Compton technique is less familiar than spin-polarized neutron diffraction a brief outline of the interpretative theory is included.

The quantity extracted from the differential scattering cross section for unpolarized radiation is the Compton profile, denoted  $J(p_z)$ : it is the projection of the electron momentum density,  $n(\mathbf{p})$  along the scattering vector which is conventionally chosen as the  $z$  direction, viz:

$$J(p_z) = \int \int n(\mathbf{p}) dp_x dp_y. \quad (1)$$

The above expression is derived within the impulse approximation which requires the energy transferred to the electron to be much greater than its binding energy; its final state is

then treated as a plane wave. The approximation is valid in the majority of Compton experiments which are performed with  $\gamma$ -ray or x-ray energies above 50 keV and at large angles of scattering.<sup>23</sup> The  $z$  axis momentum component of the electron in its ground state,  $p_z$ , can be related by simple kinematics to the energy of the photon ( $E_i$  initial,  $E_s$  final) and the angle of scattering  $\theta$ . The electron momentum is normally expressed in atomic units (a.u. where  $e = m = \hbar = 1$ ,  $c = 137$ , then 1 a.u. of momentum =  $1.99 \times 10^{-24}$  kg m s<sup>-1</sup>).

When polarized radiation is used the cross section contains a term which couples the circularly polarized component of the electromagnetic field to the spin of the electron. This term is of order  $P_c |\mathbf{K}|/mc$  where  $P_c$  is the degree of circular polarization<sup>18</sup> and  $\mathbf{K} = \mathbf{k}_i - \mathbf{k}_s$  is the conventional scattering vector,  $\mathbf{k}_i$  and  $\mathbf{k}_s$  being the incident and scattered beam wave vectors, respectively. The magnetic scattering is a measurable but small fraction of the charge scattering, amounting for example to 1% in Fe but less than 0.1% in UFe<sub>2</sub> for beams with of the order of 50% circular polarization; it can be reversed by changing the direction of magnetization or the hand of polarization, thus enabling the spin scattering to be isolated from the dominant charge-scattering contribution.

The measurement can be understood by first considering the Klein-Nishina cross section  $(d\sigma/d\Omega)_{\text{KN}}$  for radiation with defined values of linear  $P_l$  and circular  $P_c$  polarization scattered from a free, stationary electron:<sup>24</sup>

$$\left(\frac{d\sigma}{d\Omega}\right)_{\text{KN}} = \frac{1}{4} \left(\frac{e^2}{mc^2}\right)^2 \left(\frac{k_s}{k_i}\right)^2 \left[ 1 + \cos^2\theta + \frac{k_i - k_s}{mc} (1 - \cos\theta) + P \sin^2\theta - P_c (1 - \cos\theta) \frac{\boldsymbol{\sigma}(\mathbf{k}_i \cos\theta + \mathbf{k}_s)}{mc} \right], \quad (2)$$

where  $P_c$  is a positive fraction,  $P_l$ , which is negative, is  $-1$  for a beam completely linearly polarized in the scattering plane and the quality  $\boldsymbol{\sigma}$ , the spin moment is positive or negative depending on the direction of the magnetic field. The double-differential cross section for a *free-moving* electron with spin, as calculated by Bhatt *et al.*<sup>25</sup> then has the form

$$\frac{d^2\sigma}{d\Omega dE_s} = \left(\frac{2k_s}{k_i}\right) \left(\frac{m}{\hbar K}\right) \left(1 + \frac{E_i(1 - \cos\theta)}{mc^2}\right) \left(\frac{d\sigma}{d\Omega}\right)_{\text{KN}} J(p_z), \quad (3)$$

where the first three brackets on the right-hand side of the equation arise from the transformation from a momentum to an energy scale (i.e.,  $\partial p_z/\partial E_s$ , which has been approximated by its value at  $p_z=0$ ). This expression is consistent with the impulse approximation, since it treats the electron as free but moving. There are several calculations for bound electrons in the literature<sup>14,18,26–28</sup> they proceed by perturbation expansions in  $E/mc^2$  ( $=|\mathbf{K}|/mc$ ) and  $p_z/mc$  and yield a cross section that, to first order, looks exactly like the one above. The important points to note are that the cross section is linear in  $P_c$ , and scales with the momentum transfer [NB at backscattering the factor  $(\mathbf{k}_i \cos\theta + \mathbf{k}_s)$  has the magnitude of precisely  $\mathbf{K}$ , the scattering vector]. This means that magnetic Compton scattering has one difference from magnetic x-ray diffraction which arises from its incoherent nature; namely that the spin-dependent effect can be increased by studying it at higher momentum transfer, whereas in diffraction the momentum transfer is fixed for a particular Bragg reflection.

The so-called magnetic Compton profile,  $J_{\text{mag}}(p_z)$ , which is strictly speaking a spin-dependent quantity, is derived from the difference in cross sections measured when spins are reversed ( $\uparrow$  to  $\downarrow$ ), is given by

$$J_{\text{mag}}(p_z) = \int \int [n\uparrow(p) - n\downarrow(p)] dp_x dp_y. \quad (4)$$

The magnetic effect is defined by the ratio  $R$  as  $(I^+ - I^-)/(I^+ + I^-)$  where  $I^+$  and  $I^-$  represent the integrated Compton intensities for opposing sample magnetization. The data are placed on an absolute scale by calibration with a measurement on pure metallic Fe whose moment is well known at  $2.1 \mu_B$  which is almost entirely due to spin, the orbital moment being quenched. Iron also has a large magnetic effect so it needs a comparatively small counting time to achieve similar accuracy to the main investigation.

## II. EXPERIMENTAL DETAILS

The measurements were carried out at the ARNE-1 station of the Accumulation Ring Source at KEK, Japan which is equipped with an elliptical multipole wiggler and a doubly bent Si(111) silicon monochromator.<sup>29</sup> The flux at the sample was of the order of  $10^{10}$  ph s<sup>-1</sup> mm<sup>-2</sup> and the beam incident on the sample was approximately 2 mm square. The scattered intensity was detected with a 13-element Ge solid-state detector. The average energy resolution of the detectors was 0.53 keV which translates to a momentum resolution of 0.78 a.u. The additional resolution broadening due to geometrical divergence and monochromator bandwidth were negligible by comparison. Hence the experimental resolution is determined by the detector response function. The experimental method follows that employed in our previous studies of rare-earth magnetic compounds.<sup>19,20,30,31</sup>

The sample of UFe<sub>2</sub> was in the form of a single crystal of 10 mm diameter and 4 mm thick, situated 900 mm from the multielement detector. It was mounted in a displax cryostat and cooled to 20 K. The cryostat sat between the poles of an

electromagnet producing a field of 0.5 T in the gap, the field direction being aligned with the scattering vector. The field was reversed every 15 s in order to ensure good signal averaging as the beam lifetime was only a few hours.

A 25- $\mu\text{m}$  tungsten filter was placed in the scattered beam in order to reduce the x-ray fluorescence from the uranium *L* shell (13–20 keV). In the first experimental period only some 21 h of useful beamtime were available over a 3-day period;  $3.8 \times 10^9$  photons were detected but with the magnetic effect limited to 0.07% the statistical accuracy was insufficient to permit analysis of the spin moments. A second experiment, several months later, was more successful with  $2.1 \times 10^{10}$  photons detected. It is the analysis of the second data set which is reported below. The incident beam energy was 59.38 keV with a degree of circular polarization of approximately 60%. The mean scattering angle was 160° giving a Compton peak energy of 48.46 keV.

## III. DATA ANALYSIS

The procedure for transforming the experimentally measured scattering cross sections into the magnetic Compton profile has been described in earlier papers.<sup>19,20,30,31</sup> The data from each of the 13 detectors were processed independently and then individually scrutinized for anomalies. As the magnetic Compton signal is the difference spectrum obtained upon field reversal the fluorescence lines should cancel (no magnetic effect) as should the high momentum tails of the profiles ( $p_z > 10$  a.u.) because these are dominated by inner shell electrons which are spin paired. The data were corrected for energy-dependent factors associated with absorption in the sample and in the tungsten filter, the energy dependence of the detectors' efficiency, the charge and the magnetic scattering cross sections; they were then converted from an energy to a momentum scale, normalized, and finally summed.

The normalization factor was determined as follows. There is no Compton scattering contribution from the uranium *K*-shell electrons because the binding energy of 115 keV exceeds the energy of the incident energy. For Fe the *K*-shell binding energy is 7.1 keV and all 26 electrons make some contribution to the Compton scattered intensity. The effective number of electrons in UFe<sub>2</sub> from which Compton scattering can occur within a prescribed momentum range can be determined from their binding energies and tabulations of free atom profiles.<sup>32</sup> The reason why free-atom Compton profiles can be used with confidence to fit the line shapes at high momentum is because solid-state binding effects are limited to low momentum. The reason for this follows from the fact that the second moment of the profile is proportional to the kinetic energy of the electron and hence, via the virial theorem, the total energy (with a change of sign). Cohesive energies are very small compared to total energies and the changes associated with the formation of a solid are therefore necessarily restricted to low momenta. In this case for  $-10 < p_z < +10$  a.u. the effective number of electrons is 141.35. The spin moment of UFe<sub>2</sub>, used for normalization, was determined from a calibration.

Previous experience<sup>4,30,31</sup> has shown that the magnetic Compton profiles of similar rare-earth compounds can be analyzed in terms of the Fe *3d* and rare-earth *4f* contribu-

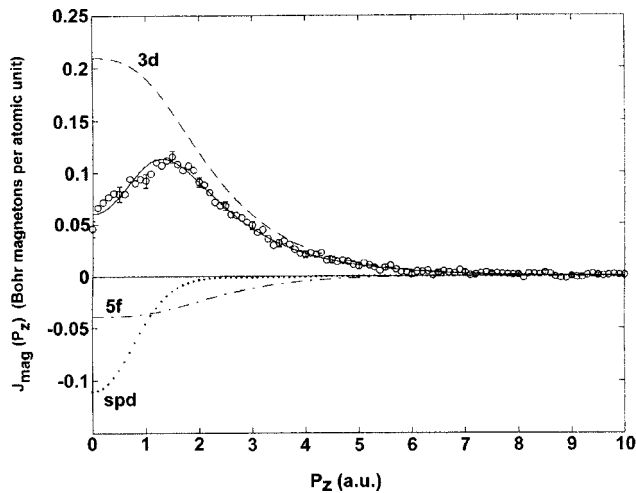


FIG. 2. The measured magnetic Compton profile of  $\text{UFe}_2$  fitted by free-atom Compton profiles (Ref. 29) for Fe  $3d$  (—), U  $5f$  (-·-·-). The diffuse component, labeled  $spd$ , is modeled as the sum of a U  $6d$  free-atom profile and a free-electron parabola smeared with the experimental resolution function. In fact, these two as fitted are almost identical in shape and cannot be separated (····). The total best-fit curve is shown as a solid line through the data points.

tions to the spin moment despite the fact that the magnetic Compton profile is the sum of all the spin contributions. The key is that the momentum distributions of electrons in transition-metal  $3d$  and rare-earth  $4f$  orbitals differ markedly. The  $4f$  electrons are more tightly bound than the  $3d$  electrons and their momentum distribution extends to higher momenta. Typically the two component Compton profiles have half widths which differ by more than 20%. Furthermore, any diffuse contribution in position space, be it a  $5d$  orbital centered on the rare earth or a delocalized conduction electron contribution, is characterized by low momenta and therefore leads to a magnetic Compton profile typically restricted to less than 2 a.u. Thus the  $3d$ ,  $4f$ , and diffuse electron contributions could be determined with a relative accuracy of a few percent.

By comparison with the rare earths the uranium  $5f$  momentum distribution is more similar to the  $3d$  momentum distribution. The  $5f$  and  $3d$  profile half widths differ by no more than 10%, compared with 20% between  $4f$  and  $3d$ , which unfortunately means that the precision of the separation is far lower. A best fit was obtained for the Fe  $3d$ , U  $5f$ , and U  $6d$  free-atom Compton profiles using the tabulated functions of Biggs, Mendelsohn, and Mann.<sup>32</sup> Figure 2 shows the synthesized line when the data are fitted over the whole momentum range out to 10 a.u. The predicted spin moments, which are simply the areas under the component curves, are shown in the table together with those deduced from neutron data and the calculated values. The best fit achieved with the component profiles leads to the moments listed in the table. The errors in the last significant digit are shown in the brackets. They are comparatively large because of the similarity between the Fe  $3d$  and U  $5f$  line shapes. If profiles derived from band, rather than free-atom, calculations were available they would differ somewhat and the estimation of the diffuse moment would change.

A word of explanation is needed with regard to the diffuse component of the spin moment labeled  $spd$  in the table and

in Fig. 2. This moment may be composed of a mixture of uranium  $6d$  electrons and truly diffuse itinerant electrons. Two approaches were tried. In the first instance the data were fitted solely with a U  $6d$  profile, although it is quite clear that not all the low-momentum electrons are localized at the uranium atom site. The uranium  $6d$  profile has a full width at half maximum of approximately 1.0 a.u. and drops to 6% of its peak value by 2.0 a.u., thus it does not dominate the data fitted by the Fe  $3d$  and U  $5f$  profiles which have half widths greater than 2.0 a.u. A second approach was to use a free-electron model for the entire diffuse component as had been adopted in the studies of the rare earths. In this case, treating the Fermi momentum as a fitting parameter, the result is the same, because the half width of the resulting profile is only 6% narrower than the uranium  $6f$  function and is zero by 2.0 a.u. Thus if both models produce partial profiles with the same enclosed area (i.e., the same partial spin moment), the method of analysis is not sensitive to the partition of the diffuse spin moment between the U  $6d$  and free-electron models. The corollary is, of course, that the line-shape analysis cannot discriminate between these separate contributions.

The second column is deduced by limiting the fitting to the momentum range 2–10 a.u. By this means the fitting is not affected at all by the nature of the delocalized electron contribution and the fact that the free-atom profiles will not describe the solid-state effects at low momenta. The diffuse moment, irrespective of its origin is then determined by the difference between the fitted component line shapes and the data in the range 0–2 a.u. Notice that a comparatively small reduction ( $\sim 10\%$ ) on Fe  $3d$  moments on each site is mirrored by the same total reduction in spin moment on uranium which amount to  $\sim 30\%$  of the value of the latter. The diffuse moment is little changed by this second fitting procedure. Comparison of our data with both neutron and MXCD results suggests that the “free fit” analysis of the Compton data (i.e., column 1 in the table) is the more appropriate alternative.

Despite the comparative imprecision of the fitting procedure relative to other investigations, the delocalized moment is approximately twice the predicted value and is insensitive to which of the two alternative methods of analysis of the Compton data are used, a result that is in agreement with neutron data. Second, the spin moment on the uranium site is not as large as the predicted value: in fact, it is less than half the calculated amount when deduced by either method of line-shape analysis. Again this result is in line with the neutron experiment. The spin moment at the iron site is only two-thirds of the predicted value. The recently published circular dichroism uranium  $M$ -edge data<sup>10</sup> provide no information about the Fe  $3d$  and the diffuse moments but confirm the virtual cancellation of the spin and orbital moments on uranium predicted by theory. The sizes of their deduced moments are however much smaller than the calculated ones in agreement with the Compton and neutron data. The MXCD results were obtained, via the sum rules, by assuming that the expectation value of the dipole moment  $\langle T_z \rangle$  is zero as it is in the itinerant transition metal ferromagnets; an assumption which appears to be validated.

The Compton results confirm the analysis of the neutron data, but by a different and possibly more direct method. As in the study<sup>31</sup> of moments in  $\text{CeFe}_2$ , it is an example of the

value of spin-dependent Compton in the study moments in ferromagnets. In both cases the calculation is quantitatively in error.

#### ACKNOWLEDGMENTS

The authors are grateful to the authorities at the KEK laboratory, Japan, for providing beamtime for this project

and to H. Kawata and other staff at KEK for their assistance. We thank G. H. Lander of EITU Karlsruhe for commenting on this manuscript and, together with J. Rebizant, for arranging for their UFe<sub>2</sub> crystal to be available to us in Japan. The project was funded by the Engineering and Physical Sciences Research Council in the UK and forms part of a research programme funded by the European Union under Contract No. ERCBCHRX CT 930135.

- <sup>1</sup>Y. F. Popov, R. Z. Levitin, M. Zeleny, A. V. Deryagin, and A. V. Andrev, *Sov. Phys. JETP* **51**, 1223 (1980).
- <sup>2</sup>M. Yessik, *J. Appl. Phys.* **40**, 1133 (1969).
- <sup>3</sup>G. H. Lander, A. T. Aldred, B. D. Dunlap, and G. K. Shenoy, *Physica B* **86-88**, 152 (1977).
- <sup>4</sup>M. Wulff, G. H. Lander, B. Lebech, and A. Delapalme, *Phys. Rev. B* **37**, 4719 (1989).
- <sup>5</sup>M. S. S. Brooks, O. Eriksson, B. Johansson, J. J. M. Franes, and P. H. Frings, *J. Phys. F* **18**, L33 (1988).
- <sup>6</sup>B. Lebech, M. Wulff, G. H. Lander, J. Rebizant, J. C. Spirlet, and A. J. Delapalme, *J. Phys. Condens. Matter* **1**, 10 229 (1989).
- <sup>7</sup>G. H. Lander and G. Aeppli, *J. Magn. Magn. Mater.* **100**, 151 (1991).
- <sup>8</sup>B. Lebech, M. Wulff, and G. H. Lander, *J. Appl. Phys.* **69**, 5891 (1991).
- <sup>9</sup>O. Eriksson, M. S. S. Brooks, B. Johansson, R. C. Albers, and A. M. Boring, *J. Appl. Phys.* **69**, 5897 (1991).
- <sup>10</sup>M. Finazzi, Ph. Sainctavit, A-M Dias, J.-P. Kappler, G. Krill, J.-P. Sanchez, P. Dalmas de Rotier, A. Yaounac, A. Rogalev, and J. Goulon, *Phys. Rev. B* **55**, 3010 (1997).
- <sup>11</sup>B. T. Thole, P. Carra, F. Sette, and G. van der Laan, *Phys. Rev. Lett.* **68**, 1943 (1992).
- <sup>12</sup>P. Carra, B. T. Thole, M. Altarelli, and X. Wang, *Phys. Rev. Lett.* **70**, 694 (1993).
- <sup>13</sup>M. J. Cooper, E. Zukowski, S. P. Collins, D. N. Timms, F. Itoh, and H. Sakurai, *J. Phys. Condens. Matter* **4**, L399 (1992).
- <sup>14</sup>P. Carra, M. Fabrizio, G. Santoro, and B. T. Thole, *Phys. Rev. B* **53**, R5994 (1996).
- <sup>15</sup>S. W. Lovesey, *J. Phys. Condens. Matter* **8**, L353 (1996).
- <sup>16</sup>N. Sakai and K. Ono, *Phys. Rev. Lett.* **37**, 351 (1976).
- <sup>17</sup>M. J. Cooper, D. Laundry, D. A. Cardwell, D. N. Timms, and R. S. Holt, *Phys. Rev. B* **34**, 5984 (1986).
- <sup>18</sup>N. Sakai, *J. Appl. Crystallogr.* **29**, 81 (1996).
- <sup>19</sup>E. Zukowski, S. P. Collins, M. J. Cooper, D. N. Timms, F. Itoh, H. Sakurai, H. Kawata, Y. Tanaka, and A. Malinowski, *J. Phys. Condens. Matter* **5**, 4077 (1993).
- <sup>20</sup>E. Zukowski, M. J. Cooper, D. N. Timms, R. Armstrong, F. Itoh, H. Sakurai, Y. Tanaka, M. Ito, H. Kawata, and R. Bateson, *J. Phys. Soc. Jpn.* **63**, 3838 (1994).
- <sup>21</sup>M. J. Cooper, E. Zukowski, D. N. Timms, R. Armstrong, F. Itoh, Y. Tanaka, M. Ito, H. Kawata, and R. Bateson, *Phys. Rev. Lett.* **71**, 1095 (1993).
- <sup>22</sup>P. K. Lawson, J. E. McCarthy, M. J. Cooper, E. Zukowski, D. N. Timms, F. Itoh, H. Sakurai, Y. Tanaka, H. Kawata, and M. Ito, *J. Phys. Condens. Matter* **7**, 389 (1995).
- <sup>23</sup>M. J. Cooper, *Rep. Prog. Phys.* **218**, 415 (1985).
- <sup>24</sup>F. W. Lipps and H. A. Tolhoek, *Physica (Amsterdam)* **20**, 85 (1954); **20**, 395 (1954).
- <sup>25</sup>G. Bhatt, H. Grotch, E. Kazes, and D. A. Owen, *Phys. Rev. A* **28**, 2195 (1983).
- <sup>26</sup>P. M. Platzman and N. Tzoar, *Phys. Rev. B* **2**, 3556 (1970).
- <sup>27</sup>H. Grotch, E. Kazes, G. Bhatt, *Phys. Rev. A* **27**, 243 (1983).
- <sup>28</sup>S. W. Lovesey, *Rep. Prog. Phys.* **56**, 257 (1993).
- <sup>29</sup>H. Kawata, T. Miyahara, S. Yamamoto, T. Shioya, H. Kitamura, S. Sato, S. Asaoka, N. Kananaya, A. Lida, A. Mikuni, M. Sato, T. Iwazumi, Y. Kitajima, and M. Ando, *Rev. Sci. Instrum.* **60**, 1885 (1989).
- <sup>30</sup>M. J. Cooper, *Physica B* **192**, 191 (1993).
- <sup>31</sup>M. J. Cooper, P. K. Lawson, M. A. G. Dixon, E. Zukowski, D. N. Timms, F. Itoh, H. Sakurai, H. Kawata, Y. Tanaka, and M. Ito, *Phys. Rev. B* **54**, 4068 (1996).
- <sup>32</sup>F. Biggs, L. B. Mendelsohn, and J. B. Mann, *Nucl. Atom. Data Tables* **16**, 201 (1975).